

Motivation: Why Detect Coronal Holes (CHs)?

As their interiors host collisionless plasmas that are expelled as the fast solar wind and their boundaries host mixed magnetic topologies that are believed to form the slow wind, CHs have **dual significance** for the **science** of solar wind formation and the **societal impacts** of space weather. Automated, pixel-wise CH detection from solar imagery enables quantitative, long-term, and high-cadence data analysis that plays a pivotal role in constraining:

- **Reconnection-Based Slow Wind Release Theories:** Evidence has mounted for interchange reconnection as a dominant mechanism, including a CH detection-based analysis of dynamics in boundary complexity [11]
- **Predictive Coronal Models:** Modeled-detected CH discrepancies have been analyzed [1] and may be algorithmically minimized to complement accuracy improvements that have been achieved with in situ solar wind [4] and white light coronal data [7]

CH Boundary Detection Challenges

The pioneering detection method of [3] using infrared He I 10830 Å images and magnetograms has paved the way for advances by dozens of Extreme Ultraviolet (EUV) image-based methods [12], but challenges remain:

- **Monochromatic Measurements of Multi-Thermal Plasma:** Open field CHs appear with similar brightness as closed field filaments in EUV and quiet Sun in He I
- **2D Imaging of 3D Structure:** Volumetric emission along an observer's line of sight may obscure underlying CH boundaries
- **Lack of Ground Truth:** Ambiguity exists in CH boundary location between optical filters, detection methods, and even expert opinions

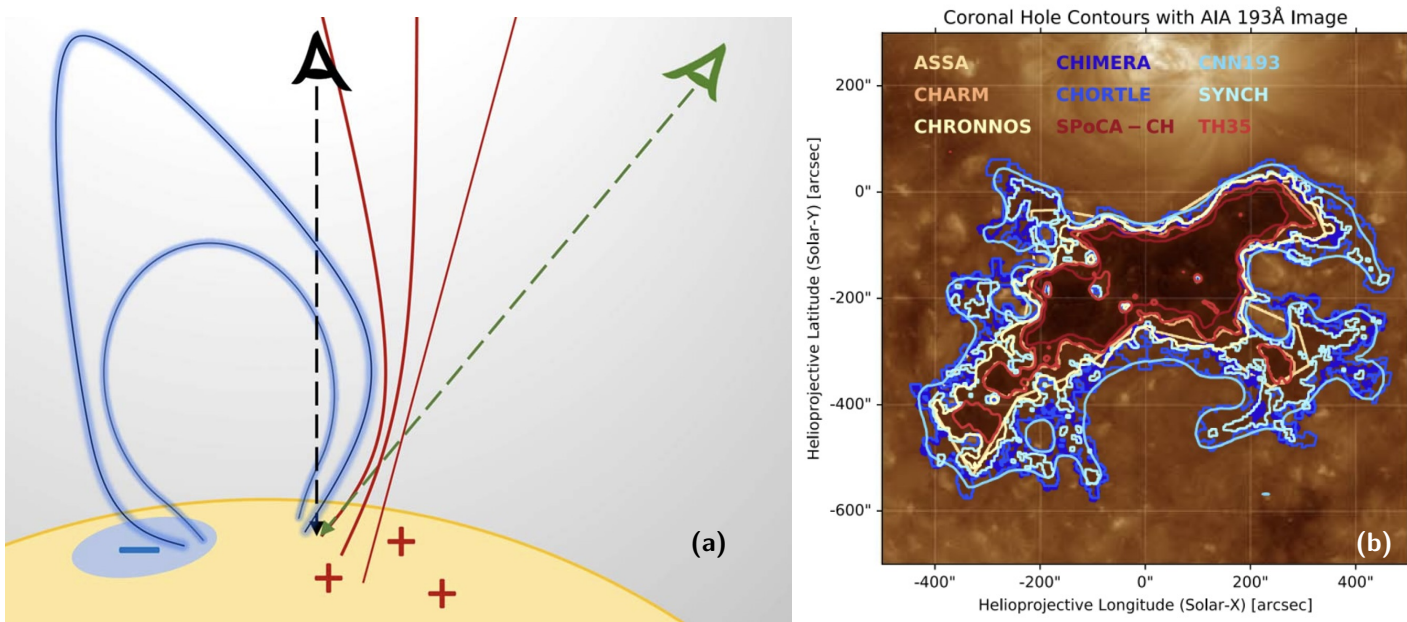


Figure 1. Depiction (a) of bright coronal loops (blue) obscuring the CH (red) along the primary observer's line of sight (black), as reproduced from [1]. The PSI-MIDM detection method [1] addresses this challenge by using near-Earth observations at a different time with a better-positioned line of sight (green). EUV 193 Å image [6] of a CH with boundaries detected by a variety of methods (b), as reproduced from [10].

CH Boundary Detection Methods

CH maps detected by the complementary methods below are fused into CH maps with Uncertainty Quantification (UQ) via pixel-wise max detection confidence.

Active Contours Without Edges (ACWE) [5]

- Ingest a space-borne EUV image sampling the **solar corona with high CH-quiet Sun contrast** and threshold for dark regions
- **Deterministic boundary adaptation** through optimization over boundary contours C to minimize variability of pixel-wise image intensities I both enclosed by and exterior to C
- **UQ** by varying the relative weighting granted to in-region homogeneity λ_i/λ_o and linearly rescaling to CH confidence

$$\min_C \lambda_i \sum_{\text{enclosed by } C} [I - \text{avg}(I)]^2 + \lambda_o \sum_{\text{exterior to } C} [I - \text{avg}(I)]^2$$

Sub-Transition Region Identification of Ensemble Coronal Holes (STRIDE-CH) [9]

- Ingest a ground-observed He I image of the **chromosphere without coronal obscuration** and threshold for bright regions^a
- **Probabilistic false positive screening** of quiet Sun through a simple statistical learning model^b trained to favor high unipolarity U , smoothness in He I S , and proximity to disk center p
- **UQ** by linearly rescaling the predicted probability of being a CH, conditioned on the region's features, to CH confidence

$$P(\text{CH} | \mathbf{x} = [U \ S \ p]^T) \in [P_{\text{thresh}}, 1] \mapsto \text{Confidence} \in [0, 1]$$

Limitations: ACWE is liable to detect filaments due to a lack of magnetic field constraints and He I images are available only at a daily cadence and up to 2015 for STRIDE-CH

^aBoundaries are then reshaped with morphological operations and an ensemble of detections is made with varied threshold levels and structuring element sizes

^bBayesian linear discriminant analysis trained/tested on 140/153 labeled regions in 2012/2015, with 6 testing dates being from the benchmark dataset developed by [12]

Flowchart To Fuse Observations

We present an image segmentation method for CHs aiming to:

- Disambiguate similar brightness, non-CH, structures with **multi-spectral imagery**
- Stride past coronal obscuration with **imagery across solar atmospheric heights**
- Address the lack of ground truth through **accurate uncertainty quantification**

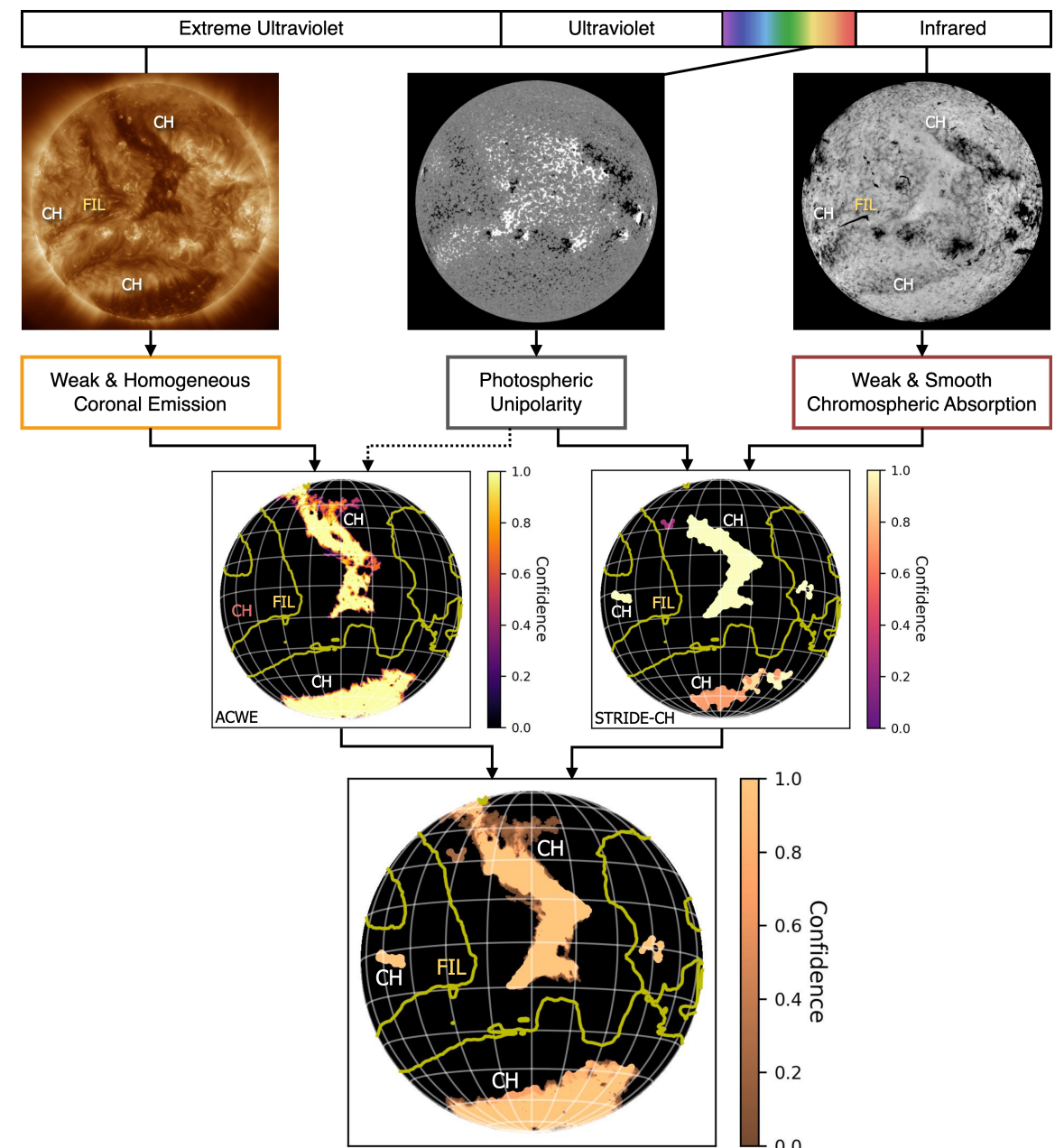


Figure 2. Observations on March 31, 2015 in EUV 193 Å [6], visible 6302 Å magnetogram [8], and He I 10830 Å [8] that each sample the corona, photospheric magnetic field, and the chromosphere. CH detections from ACWE and STRIDE-CH are fused into a final confidence map. The integration of magnetic data into ACWE, indicated by the dashed arrow, is an area for future work. Yellow contours indicate large-scale magnetic polarity changes where CHs may not occur.

- Filaments (e.g. that labeled 'FIL') are correctly rejected due to unipolarity constraints
- Polar CH boundaries are detected well in EUV due to increased CH-quiet Sun contrast
- CHs obscured in EUV (e.g. the leftmost CH) are **detected earlier and for extended periods** as the Sun rotates in He I due to the absence of coronal emission

Improved Classification & Uncertainty Quantification (UQ)

A desirable variance reduction in detection confidence for highly certain regions (labeled true/false) and an increase in variance for uncertain regions (labeled marginal) are demonstrated in the box plot.

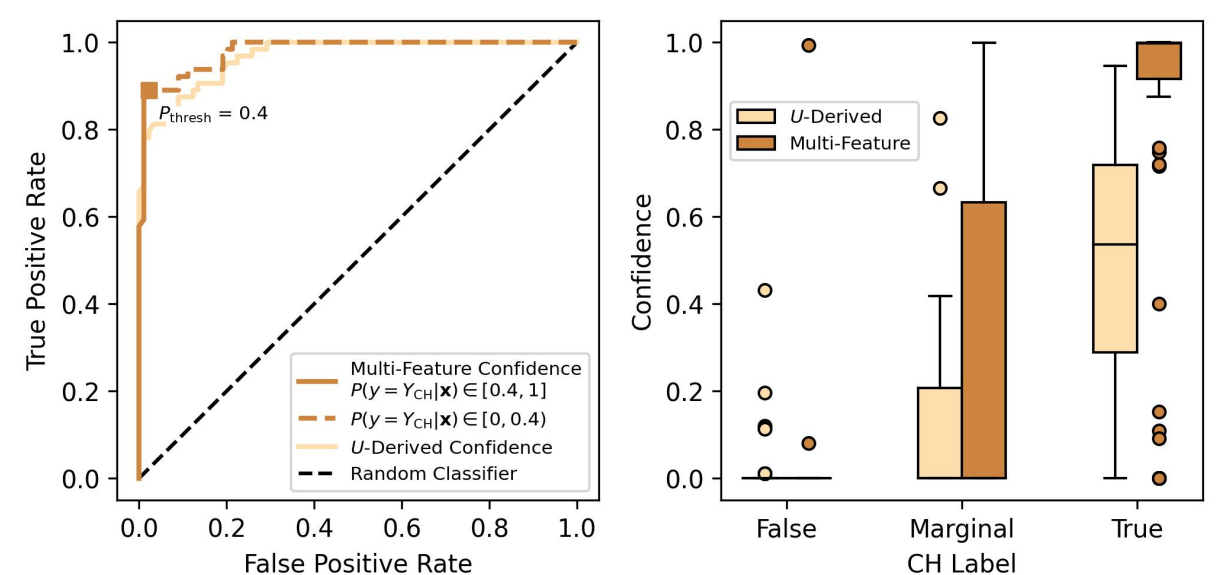


Figure 3. STRIDE-CH binary classification curves and detection confidence vs. region label box plots are compared between the "Multi-Feature" method for deriving confidence, as described in the Methods section, and "U-Derived" which relies on unipolarity U alone as proposed in [9]. They are both evaluated on 20 dates in 2015 that extrapolate from the 2012 training dataset for the "Multi-Feature" method.

Future Work: Fuse STRIDE-CH with magnetic field-constrained ACWE [2] and apply such data-derived constraints to optimize predictive coronal models

References

- [1] R. M. Caplan et al. *Astrophys. J.* (Nov. 2023). DOI: 10.3847/1538-4357/ad01b6.
- [2] J. A. Grajeda et al. *arXiv e-prints* (Jan. 2025). DOI: 10.48550/arXiv.2501.13211.
- [3] C. J. Henney et al. *Astron. Soc. Pac. Conf. Ser.* Dec. 2005. DOI: 10.48550/arXiv.astro-ph/0701122.
- [4] O. Issan et al. *Space Weather* (Sept. 2023). DOI: 10.1029/2023SW003555.
- [5] J. A. Grajeda et al. *Sol. Phys.* (Nov. 2023). DOI: 10.1007/s11207-023-02228-0.
- [6] J. R. Lemen et al. *Sol. Phys.* (Jan. 2012). DOI: 10.1007/s11207-011-9776-8.
- [7] S. I. Jones et al. *Astrophys. J.* (June 2020). DOI: 10.3847/1538-4357/abf2c8.
- [8] C. U. Keller et al. Ed. by M. Sigwarth. *Astron. Soc. Pac. Conf. Ser.* Jan. 2001.
- [9] J. A. Landeros et al. *Sol. Phys.* (Jan. 2025). DOI: 10.1007/s11207-024-02416-6.
- [10] M. A. Reiss et al. *Astrophys. J.* (May 2021). DOI: 10.3847/1538-4357/abf2c8.
- [11] E. I. Mason et al. *Astrophys. J. Lett.* (Sept. 2022). DOI: 10.3847/2041-8213/ac9124.
- [12] M. A. Reiss et al. *Astrophys. J. Suppl.* (Mar. 2024). DOI: 10.3847/1538-4365/ad1408.